Tinoco, I., Jr., Halpern, A., & Simpson, W. T. (1962) in *Polyamino Acids, Polypeptides, and Proteins* (Stahmann, M. A., Ed.) pp 147–160, University of Wisconsin Press, Madison, WI.
Trulson, M. O., & Mathies, R. A. (1986) *J. Chem. Phys. 84*, 2068.
Walton, A. G. (1981) *Polypeptides and Protein Structure*, pp 172–188, Elsevier, New York.
Wand, A. J., & Englander, S. W. (1986a) *Biochemistry 25*, 1100.
Wand, A. J., & Englander, S. W. (1986b) *Biochemistry 25*, 1107.
Wetlaufer, D. B. (1962) *Adv. Protein Chem. 17*, 303.
Williams, R. W. (1983) *J. Mol. Biol. 166*, 581.
Williams, R. W., & Teeter, M. M. (1984) *Biochemistry 23*, 6796.

Interaction of Polymyxin B Nonapeptide with Anionic Phospholipids†

Peter Kubesch,‡ Joan Boggs,§ Liliana Luciano,‖ Günter Maass,‡ and Burkhard Tümmler*,‡

Abteilung Biophysikalische Chemie and Abteilung Zellbiologie und Elektronenmikroskopie, Medizinische Hochschule, D-3000 Hannover 61, West Germany, and Research Institute, Department of Biochemistry and of Clinical Biochemistry, The Hospital for Sick Children, Toronto, Ontario, Canada M5G 1X8

Received August 14, 1986; Revised Manuscript Received December 11, 1986

ABSTRACT: The interaction of polymyxin B nonapeptide (PMBN) and polymyxin B (PMB) with the anionic phospholipids phosphatidylserine (PS), dipalmitoylphosphatidylglycerol (DPPG), dipalmitoylphosphatidic acid (DPPA), and 1:1 mixtures (w/w) of DPPA and distearoylphosphatidylcholine (DSPC) was studied by calorimetry, electron spin resonance, and fluorescence spectrometry, electron microscopy, and fusion and leakage assays. The phase transition temperatures of DPPA and DPPG were very similar when bound to PMB or PMBN, indicating that the lipids are in a similar state when bound to the cationic peptides. Both PMB and PMBN caused the interdigitation of DPPG bilayers, suggesting that the penetration of hydrophobic side chains from a peptide bound electrostatically on the surface is sufficient to induce this phenomenon. Stopped-flow experiments revealed that PMBN and PMB induced the fusion of small unilamellar PS and large unilamellar DPPA–DSPC vesicles. The aggregation of vesicles was found to be a diffusion-controlled process; the subsequent fusion took place with a frequency of 10^2–(5×10^2) s^{-1} for small vesicles and 1–100 s^{-1} for large vesicles. The freeze–fracture replicas of the PMB-treated vesicles displayed 12–50-nm depressions on several superimposed bilayers, indicating the formation of stable lipid–PMB domains. Since the incubation with PMBN produced similar depressions only if the specimens were fixed, PMBN-induced domain formation seems to be a reversible rapid process. The differences in the phospholipid–peptide interactions are correlated with the differences in the physiological action of the antibiotic PMB and the nonbactericidal PMBN on the cell envelope of Gram-negative bacteria.

The cationic peptide polymyxin B nonapeptide (PMBN)[1] is a derivative of the antibiotic polymyxin B that lacks the fatty acyl part of the parent compound (Chihara et al., 1973). PMBN is not bactericidal; however, it sensitizes Gram-negative bacteria to other amphiphilic and hydrophobic compounds (Vaara & Vaara, 1983b–d; Viljanen & Vaara, 1984). In the presence of PMBN, Gram-negative bacteria become vulnerable to a wide range of antimicrobial agents to which they were previously insensitive because the restrictive permeability properties of the outer membrane are lost (Vaara & Vaara, 1983c; Nikaido & Vaara, 1985).

PMBN and polymyxins are compounds to which the presence of five or six 2,4-diaminobutyric acid residues confers a net positive charge. In the case of the polymyxins, binding to acidic molecules of the outer membrane of Gram-negative bacteria, including the lipid A region of lipopolysaccharide (LPS), is assumed to be the primary event of drug action (Teuber & Bader, 1976; Storm et al., 1977; Hancock, 1984). Binding studies with isolated LPS (Bader & Teuber, 1973; Schindler & Osborn, 1979) and with lipid monolayers (Rosenthal et al., 1976; Teuber & Miller, 1977; El Mashak & Tocanne, 1980) and bilayers (Hartmann et al., 1978; Sixl & Galla, 1979, 1980, 1982; Galla & Trudell, 1980; Ranck & Tocanne, 1982; Boggs & Rangaraj, 1985) have revealed a high and specific affinity of the polymyxins for lipopolysaccharides and acidic phospholipids.

†This work was supported by a grant from the Deutsche Forschungsgemeinschaft. This paper is dedicated to Dr. Manfred Eigen on the occasion of his 60th birthday.

‡Abteilung Biophysikalische Chemie, Medizinische Hochschule, Hannover.
§Research Institute, The Hospital for Sick Children, Toronto.
‖Abteilung Zellbiologie and Elektronenmikroskopie, Medizinische Hochschule, Hannover.

[1] Abbreviations: CD, circular dichroism; CF, 5-carboxyfluorescein; DPA, dipicolinic acid; DPH, diphenylhexatriene; DPPA, 1,2-dipalmitoyl-*sn*-glycero-3-phosphatidic acid; DPPG, 1,2-dipalmitoyl-*sn*-glycero-3-phosphoglycerol; DSPC, 1,2-distearoyl-*sn*-glycero-3-phosphocholine; LPS, lipopolysaccharide; PMB, polymyxin B; PMBN, polymyxin B nonapeptide; PG, phosphatidylglycerol; PS, phosphatidylserine; TES, *N*-[tris(hydroxymethyl)methyl]-2-aminoethanesulfonic acid; T_m, midpoint temperature of a phase transition; EDTA, ethylenediaminetetraacetic acid; DSC, differential scanning calorimetry; Hepes, *N*-(2-hydroxyethyl)piperazine-*N*′-2-ethanesulfonic acid; ESR, electron spin resonance; Tris, tris(hydroxymethyl)aminomethane; MICs, minimum inhibitory concentrations.

0006-2960/87/0426-2139$01.50/0

In the case of PMBN, it has been suggested from the results of indirect bioassays (Vaara, 1983) and ESR experiments on the displacement of cationic spin probes (Peterson et al., 1985) that PMBN causes the disorganization of the outer membrane of Gram-negative bacteria by binding to the anionic groups of LPS. The role of the anionic phospholipids, however, remains to be elucidated. This paper focuses on the interaction of PMBN and its parent compound polymyxin B with anionic phospholipids which was studied with model membranes by employing probes of membrane fluidity, fusion, and leakage assays, freeze–fracture electron microscopy, and differential scanning calorimetry.

Materials and Methods

Chemicals. Dipalmitoylphosphatidic acid (DPPA, purum, Fluka or Calbiochem), bovine brain phosphatidylserine (PS, Sigma), distearoylphosphatidylcholine (DSPC, purissimum, Fluka), diphenylhexatriene (DPH, purissimum, Fluka), dipicolinic acid (DPA, Sigma), 5-carboxyfluorescein (CF, Calbiochem), 5-doxylstearic acid and 16-doxylstearic acid (Syva), lipopolysaccharide B from *Salmonella typhimurium* (Difco), erythromycin (Sigma), lincomycin (Sigma), cloxacillin (Sigma), fusidic acid (Sigma), nalidixic acid (Sigma), and polymyxin B sulfate (PMB, Sigma) were used as obtained from the manufacturer. Dipalmitoylphosphatidylglycerol (DPPG, purissimum) was a gift from H. J. Eibl, Göttingen, FRG, or purchased from Calbiochem. The lipids ran as one spot in thin-layer chromatography; contaminations by lysolipid or free fatty acids were not detectable. A spin-labeled phosphatidylglycerol with stearic acid esterified to the 1-OH of glycerol, and 16-doxylstearate to the 2-OH, was a kind gift from Dr. A. Watts, University of Oxford. Unless otherwise stated, all inorganic reagents and all solvents were of at least analytical grade.

Preparation of Polymyxin B Nonapeptide (PMBN). PMBN was obtained from polymyxin B by hydrolysis with ficin (Chihara et al., 1973; Vaara & Vaara, 1983a). Four

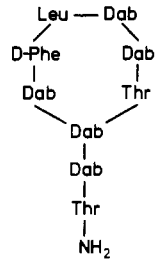

PMBN

grams of a crude preparation of ficin (Sigma) was freed from contaminating latex particles by centrifugation, ammonium sulfate precipitation, and dialysis. The final product contained about 20% ficin (yield 31%) as determined by the kinetics of the hydrolysis of benzoyl-L-arginine *p*-nitroanilide hydrochloride (Englund et al., 1968). The PMB preparation was found to be more than 98% pure by thin-layer chromatography on precoated silica gel silanized plates (Merck) [solvent: 25% acetone (v/v), 75% 0.1 N HCl (v/v), and 1% NaCl (w/v); visualization of spots by ninhydrin] (Thomas & Holloway, 1978).

One-half gram of polymyxin B sulfate was dissolved in 25 mL of 0.01 M potassium phosphate buffer, pH 7.0. After the addition of 60 mg of ficin preparation, the solution was incubated for 24 h at 37 °C with light stirring. To follow the time course of the reaction, samples of 50 μL were taken after 0, 2, 4, 8, and 24 h. The subsequent analysis revealed that the enzymatic reaction was complete after 6 h. After 24 h, the reaction mixture was boiled for 5 min at 90 °C, and the denatured enzyme was removed by centrifugation (20 min, 12000*g*). The fatty acyl diaminobutyric acid and unreacted polymyxin B were separated by extraction. The supernatant was acidified with 1 N HCl to pH 2.0, extracted 3 times with 12 mL of 1-butanol, adjusted with 1 N NaOH to pH 8, and extracted again twice with 1-butanol. The aqueous phase (V = 16.5 mL) was poured on an Amberlite IRA-410 column (OH type, 1.5 × 8.5 cm) and eluted with distilled H_2O (v = 0.25 mL/min). The first two fractions (25 mL) containing the product PMBN were lyophilized. The contamination of the PMBN preparations by polymyxin B was determined from thin-layer chromatography on cellulose-coated aluminum foil [solvent: 1-butanol/pyridine/acetic acid/H_2O, 30:20:6:24 (v/v)].

Model Membrane Studies. (A) Vesicle Preparations. For the preparation and storage of vesicle dispersions, the glassware was extensively rinsed with acetone, methanol, EDTA solutions, distilled water, and triple quartz-distilled water. At all times, the preparations were maintained at least 10 °C above T_m. Small unilamellar vesicles were prepared according to Herrmann et al. (1984) by sonication following a modification of Huang's procedure (1969). The contamination by large multilamellar vesicles was checked by plotting the turbidity between 300 and 700 nm vs. the reciprocal fourth power of the scattering wavelength (Barrow & Lentz, 1980). Large unilamellar vesicles were prepared by injection of 10 μmol of phospholipid dissolved in 5 mL of methanol/diethyl ether (1:4 v/v) into 4 mL of 0.1 M phosphate buffer, pH 7.0 (Parce et al., 1978).

For the leakage and fusion assays, small phosphatidylserine (PS) and large unilamellar DPPA–DSPC vesicles were prepared essentially as described by Wilschut et al. (1980, 1985), Fraley et al. (1980), and Sundler and Papahadjopoulos (1981). In brief, 100 μmol of PS was dispersed in 10 mL of aqueous buffer of 2 mM histidine and 2 mM *N*-[tris(hydroxymethyl)methyl]-2-aminoethanesulfonic acid (TES), pH 7.4, which contained in addition either (a) 70 mM CF, (b) 15 mM $TbCl_3$/150 mM sodium citrate, or (c) 150 mM DPA. The dispersion was sonicated for 1 h in an ice bath under nitrogen. Large particles were subsequently removed by centrifugation at 97000*g* for 1 h. Vesicles were separated from nonencapsulated material by gel filtration on Sephadex G-75 [elution buffer: 100 mM NaCl, 2.0 mM L-histidine, 2.0 mM TES, and 1 mM EDTA, pH 7.4 (0.1 mM EDTA in the case of CF vesicles)]. Large DPPA–DSPC vesicles were prepared by injection (Parce et al., 1978). In order to prevent Tb^{3+} binding to phosphatidate, the following solutions were used: 2.5 mM $TbCl_3$, 100 mM nitrilotriacetic acid, 2 mM L-histidine, and 2 mM TES, pH 7.4; 100 mM DPA, 2 mM L-histidine, and 2 mM TES, pH 7.4; 50 mM CF, 0.1 M NaCl, 0.1 mM EDTA, 2 mM L-histidine, and 2 mM TES, pH 7.4. The elution buffer contained 0.2 M NaCl, 1 mM EDTA (0.1 mM EDTA for CF vesicles), and 10 mM sodium tetraborate, pH 9.0.

For calorimetry and ESR experiments, the lipid was labeled with the fatty acid spin-label by combining chloroform/methanol solutions of lipid and spin-label at a 200:1 mole ratio and evaporation of the solvent under nitrogen. An aqueous solution of PMBN (0.81 μmol/mL) in 10 mM Hepes buffer at pH 7.4 was added to the dry film of lipid and spin-label. Multilamellar vesicles were formed by vortex dispersion at a temperature above the lipid phase transition temperature. The lipid concentration was 4 μmol/mL. The sample was divided into two parts for calorimetry and ESR measurements; the

amount of spin-label used has been found not to affect the calorimetric results. Both samples were centrifuged in an Eppendorf bench centrifuge. The wet pellet was loaded into an aluminum DSC pan for calorimetry. All but about 100 μL of the supernatant was removed from the other sample, and about 50 μL of the lipid suspension was loaded into a 100-μL capillary tube for ESR measurements, sealed with a flame at one end, and centrifuged at 2000 rpm.

(*B*) *Differential Scanning Calorimetry*. Samples were run on a Perkin-Elmer DSC-2 equipped with a data station, at heating and cooling rates of 1.25–10 °C/min. The temperature of maximum heat absorption was defined as the phase transition temperature, T_m.

(*C*) *Equilibrium Studies with DPH*. For the cooling curves, the unilamellar vesicle dispersions in 10 mM sodium tetraborate buffer, pH 9.0, were diluted to 0.5 mM phospholipid; 2.5 μL of a 2 mM DPH stock solution in tetrahydrofuran was added during rapid vortexing to 5 mL of the phospholipid dispersion. Dye and vesicles were equilibrated for 90 min at 60 °C, and then an aliquot of the PMB or PMBN stock solution was added to give 20 mol % peptide with respect to lipid. The cooling curve was recorded with a rate of 0.3 °C min^{-1} monitoring the fluorescence anisotropy of DPH (λ_{ex} = 367 nm, λ_{em} = 427 nm). Fluorescence cuvettes equipped with a water jacket were used which allowed control of the temperature to within 0.03 °C by circulating water through the cuvette and the thermostated cell holders.

The stoichiometry and stability of the PMBN–DPPA complexes were evaluated from fluorometric titrations measuring the change of anisotropy of DPH. The vesicle solution which contained DPH in a lipid to probe ratio of 50:1000 was cooled from 70 to 40 °C within 1 h. The lipid dispersion was equilibrated at 40 °C for another 2 h, and then aliquots of a PMBN stock solution were added in intervals of 20–30 min. The data were evaluated by a nonlinear curve-fitting procedure as described previously (Tümmler et al., 1979).

(*D*) *Electron Spin Resonance Experiments*. ESR spectra were measured on a Varian E-104B spectrometer (microwave power 10 mW) equipped with a Varian temperature controller and a DEC LSI-11 based microcomputer system. The maximum hyperfine splitting, T_{max}, of the ESR spectra or the motional parameter, τ_0, was measured as described earlier (Boggs et al., 1981).

(*E*) *Fusion and Leakage Assays*. Vesicle dispersions of PS or DPPA–DSPC encapsulated with Tb, DPA, or CF were mixed with solutions of PMB or PMBN in a home-built stopped-flow apparatus. The lipid concentrations were varied in the range of 0.2–1 mM for the large vesicles and in the range of 2–10 mM for the small vesicles. Taking the oxidation of ascorbic acid as the indicator reaction, the dead time of the instrument was determined to be 3 ms. The Tb–DPA complex was excited at 276 nm and CF at 430 nm, and fluorescence was measured at >515 nm through a cutoff filter (Wilschut et al., 1980, 1981, 1985).

The time course of the formation of the fluorescent Tb–DPA complex indicating vesicle fusion was analyzed according to the theory developed by Nir et al. (1980) and Bentz et al. (1983a,b). The fusion process occurs via two distinct, kinetically coupled steps. The aggregation of vesicles is followed by fusion. The process of deaggregation of aggregated vesicles can be ignored (Wilschut et al., 1985). The rate constants were evaluated from the initial time range when mostly dimers are formed. The observed Tb–DPA fluorescence, $F(t)$, was corrected for the release of vesicle contents, $D(t)$, measured by the leakage of carboxyfluorescein. During the early stages of vesicle fusion of the monomers, $D(t)$ was small compared to $F(t)$ (0–20%). The rate constants for vesicle aggregation, c_{11} (M^{-1} s^{-1}), and for fusion, f_{11} (s^{-1}), were calculated from the experimental curves by a combined simulation and iteration procedure using the formula (Bentz et al., 1983a):

$$F_{cor}(t) = 100A(t)J(t) \quad (1)$$

where

$$A(t) = (1 + 4c_{11}X_0)^{0.25} - 1 \quad (2)$$

and

$$J(t) = 1 - [1 - \exp(-f_{11}t)]/f_{11}t \quad (3)$$

X_0 is the initial molar concentration of the vesicles. The number of lipid molecules per vesicle was assumed to be 4000 for a small 25-nm unilamellar vesicle and to be 80000 for a large 100-nm unilamellar vesicle (Wilschut et al., 1980a).

(*F*) *Freeze–Fracture Electron Microscopy*. DPPA–DSPC vesicle dispersions in 10 mM sodium tetraborate buffer, pH 9.0, were incubated for 20–30 min with either 20 mol % or 50 mol % PMB or PMBN at 20 or 40 °C; some of the samples incubated at 20 °C were fixed for 1 h in 2% glutaraldehyde dissolved in 10 mM Hepes/Tris buffer, pH 7.4. Samples lacking incubation with PMB or PMBN were used as controls. Drops of each sample were rapidly frozen in liquid Freon 22 and then fractured and replicated in a Balzer 30 M apparatus supplied with a quartz crystal thin-film monitor QSG 201 (Balzer AG, Liechtenstein). Replicas of about 2.3-nm thickness were examined in a Siemens 101 electron microscope.

Microbiological Assays. The *Escherichia coli* and *Pseudomonas aeruginosa* strains were clinical isolates from wards of the Medizinische Hochschule Hannover; 1-mL aliquots of first subcultures in trypticase soy broth/glycerol (85:15 v/v) were stored at −70 °C until use. The minimum inhibitory concentrations (MICs) of antimicrobial agents in the presence and absence of PMBN were measured as follows: A solution of 0.85 mL of trypticase soy broth, pH 7.5, 0.1 mL of PMBN, and 1 mL of antibiotic in physiological saline solution was inoculated with 50 μL of the bacterial suspension which was equivalent to (2–10) × 10^7 colony forming units. The concentrations of antibiotic were varied in steps of two. The titrations were performed in triplicate. The tubes were incubated at 37 °C for 24 h. The lowest concentration of antibiotic that completely inhibited visible growth was recorded and interpreted as the MIC. The accuracy of the killing end point was controlled by viable counts.

Results

Preparation of PMBN. According to colorimetric assays with the Sanger reagent 2,4-dinitrofluorobenzene, PMBN was obtained in more than 80% yield. Thin-layer chromatography revealed that the PMBN preparations were contaminated to less than 1% by the parent compound PMB. In the difference ^1H NMR spectra of equal molar amounts of PMB and PMBN, the remaining positive resonances corresponded with the spectrum of fatty acyl diaminobutyric acid. The spectrum verified that ficin had solely cleaved the peptide bond between threonine and the diaminobutyric acid residue adjacent to the fatty acyl chain.

Microbiological Assays. The PMBN preparations were tested for their effect on the susceptibility of *Escherichia coli* and *Pseudomonas aeruginosa* to antimicrobial agents. The minimum inhibitory concentrations (MICs) of polymyxin B were determined to range between 0.1 and 0.2 μg/mL for the two *E. coli* test strains and between 1 and 2 μg/mL for the five *P. aeruginosa* test strains. The MIC values of the PMBN

Table I: Sensitization of Gram-Negative Bacteria to Antimicrobial Agents by PMBN

antimicrobial agent	sensitization index[a]	
	E. coli[b]	*P. aeruginosa*[b]
cloxacillin	5–10	5–10
erythromycin	50–200	20–100
fusidic acid	50–200	100–5000
lincomycin	2–8	2–8
nalidixic acid	5–20	50–1000

[a] The sensitization index is defined as the ratio of the minimum inhibitory concentrations in the absence and presence of 3 μg/mL PMBN. [b] Two *E. coli* and five *P. aeruginosa* strains were tested in triplicate.

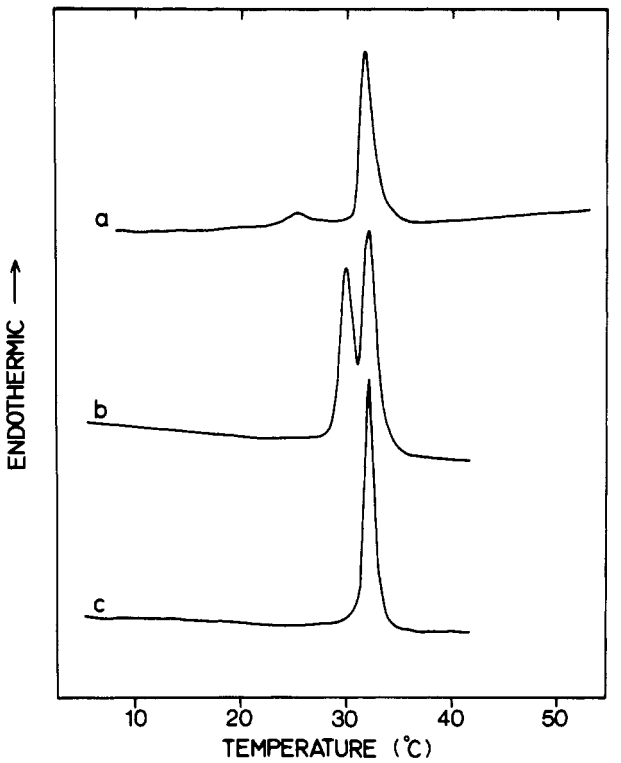

FIGURE 1: Differential scanning calorimetry of (a) DPPG only, (b) DPPG plus 20 mol % PMB, and (c) DPPG plus 20 mol % PMBN. All are heating scans at 10 °C/min. Sensitivity settings in millicalories per second were (a) 1.5, (b) 2.0, and (c) 1.5. Different amounts of lipid were in the pans so the peak areas cannot be compared.

preparations of 10–20 and 30–40 μg/mL, respectively, are indicative of less than 1% contamination by polymyxin B, in agreement with the results of thin-layer chromatography.

The PMBN preparations sensitized the bacterial strains to antimicrobial agents (Table I). The effect was rather small for the relatively hydrophilic molecules lincomycin and cloxacillin. On the other hand, in accordance with the results reported by Vaara and co-workers for a variety of other Gram-negative bacteria like *S. typhimurium* (Vaara & Vaara, 1983a,b; Viljanen & Vaara, 1984), PMBN was remarkably active in sensitizing all strains to the hydrophobic antibiotics erythromycin and fusidic acid. Nalidixic acid was found to be an interesting case. *E. coli* is usually susceptible and *P. aeruginosa* resistant to nalidixic acid (King et al., 1984). In the presence of a 3 μg/mL sample of the outer membrane perturbing PMBN, the MIC values for the *E. coli* strains decreased by approximately 1 order of magnitude and those for the *P. aeruginosa* strains by more than 2 orders of magnitude into the therapeutic range of 0.2–10 μg/mL. The PMBN-sensitized *P. aeruginosa* strains became nearly as susceptible to nalidixic acid as the *E. coli* strains. This experimental finding suggests that differences in outer membrane permeability are primarily responsible for the variations in susceptibility to nalidixic acid between the sensitive *E. coli* and the resistant *P. aeruginosa* strains.

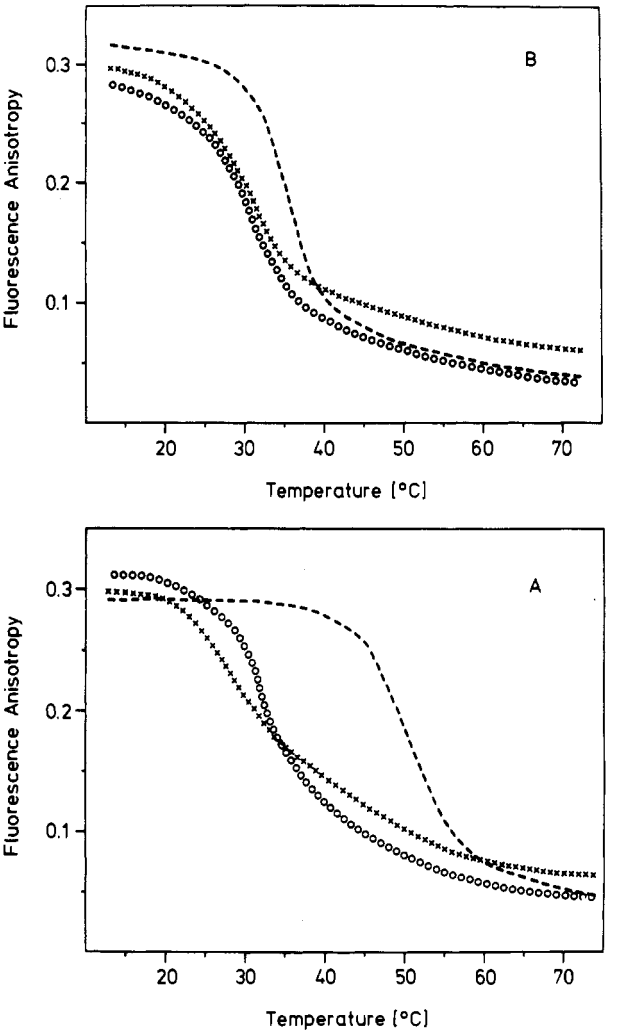

FIGURE 2: Temperature dependence of the fluorescence anisotropy of DPH incorporated into sonicated vesicles of DPPA (A) and DPPG (B): phospholipid only (dashed line); phospholipid plus 20 mol % PMB (crosses); phospholipid plus 20 mol % PMBN (circles).

Phase Transitions of DPPA and DPPG in the Presence of PMB and PMBN. (A) Calorimetry. Twenty mole percent PMB causes the appearance of two transitions for DPPG, one 1.5 °C below and one 0.5 °C above the T_m of pure DPPG (Figure 1a,b). The total enthalpy is 2 kcal/mol greater than that of the pure lipid (Boggs & Rangaraj, 1985). However, in the presence of 20 mol % PMBN, there is only a single transition at a similar temperature as the second transition for PMB (Figure 1c). A lower temperature shoulder on the main transition was observed on the first heating scan (not shown) but not on subsequent heating scans.

In the case of DPPA at pH 9, there were three transitions in the presence of 20 mol % PMB, as reported by Sixl and Galla (1982). Two of these are 19 and 22 °C below and the third is similar to the T_m of the pure lipid (Table II). PMBN, however, caused only a single transition at a temperature 18 °C below the T_m of the pure lipid (Table II). Note that the temperature of this transition of PMBN–DPPA is very close to that of PMBN–DPPG, in spite of the large difference in T_m's of pure DPPG and DPPA.

(B) DPH Fluorescence Anisotropy. In the case of DPPA, the temperature dependence of the fluorescence polarization

Table II: Phase Transition Temperatures Determined by Calorimetry

	peak temp (°C)[a]		
DPPG			41.7
DPPG–PMB		40.2	42.3
DPPG–PMBN			42.1
DPPA			58.5
DPPA–PMB	36.1	39.3	59.3
DPPA–PMBN		41.1	

[a] At a heating rate of 10 °C/min. At pH 6 for DPPG and pH 9 for DPPA. PMB and PMBN used at a concentration of 20 mol %.

of DPH indicated that 20 mol % PMBN lowered the T_m by 18 °C without affecting the half-width (Figure 2A), in agreement with the calorimetric results; 20 mol % PMB induced a comparable, but slightly more, distinct shift of the transition temperature; however, in addition the transition was broadened and became asymmetric (Figure 2A). In reference to the calorimetric data, the asymmetry of the experimental curve may be explained by the superposition of at least two separate transitions which were not clearly resolved by DPH fluorescence anisotropy. In contrast to the calorimetric results, the DPH cooling curves indicated in the case of DPPG that both 20 mol % PMBN and PMB shifted the phase transition temperature of sonicated DPPG vesicles by 5 °C to lower temperatures. The half-width of the transition remained invariant (Figure 2B). Differences in the experimental design may be responsible for the different results. For calorimetry, DPPG was dispersed in the presence of PMB and PMBN which guaranteed that the peptides were on both sides of the bilayer. In contrast, for the DPH cooling curves, the peptides were added after the preparation of sonicated vesicles.

Binding Curves of PMBN to DPPA Vesicles. The stoichiometry and stability of the PMBN–DPPA complex at 40 °C were determined from titrations of phospholipid as a function of PMBN concentration by monitoring the decrease of fluorescence anisotropy of DPH. According to the evaluation of the binding curves, 1 PMBN molecule binds 8 ± 1 DPPA molecules at pH 9.0 with an overall association constant of (1 ± 0.5) × 10^4 M^{-1}; i.e., the 5 positive charges of the peptide interact with 14–18 negative charges of phospholipid. If phospholipid was chosen in molar excess over peptide, 50% of maximal binding of PMBN to DPPA was correspondingly obtained with 12 μM PMBN. At the same pH and ionic strength, the concentration of 50% binding of polymyxin B to DPPA was measured to be 5 μM PMB (Sixl & Galla, 1979), indicating that the affinity of DPPA is about 2.5 times higher for PMB than for PMBN. In contrast to the results reported for PMB by Sixl and Galla (1979), no cooperativity was observed for the interaction of the polymyxin derivative PMBN with phosphatidic acid at pH 9 and 0.03 M ionic strength.

ESR Data. Twenty mole percent PMB has been shown by X-ray diffraction to produce an interdigitated bilayer in DPPG (Ranck & Tocanne, 1982). This results in a marked decrease in mobility and/or an increase in order of the ends of the fatty acid chains as detected with a fatty acid spin-labeled near the terminal methyl, 16-doxylstearate (Boggs & Rangaraj, 1985). Twenty mole percent PMBN had a similar effect on the spectrum of 16-doxylstearate as shown in Figure 3C. The T_{max} value in the presence of PMBN at 9 °C was 30.2 G, similar to that for PMB–DPPG (Figure 3B), and considerably greater than that of 24 G found for pure DPPG (Figure 3A). PMB and PMBN also caused a similar degree of immobilization of a phosphatidylglycerol spin-label containing 16-doxylstearate (data not shown but were available to the editors). These results suggest that PMBN, like PMB, also causes interdigitation of DPPG.

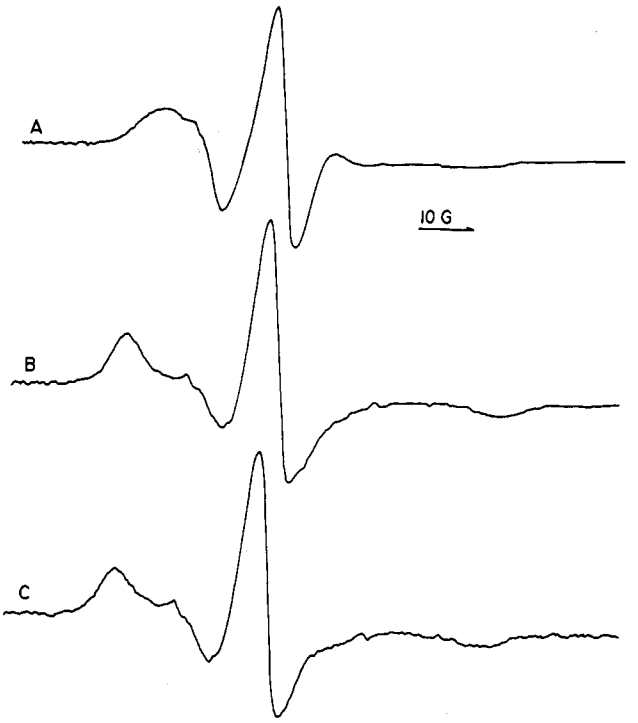

FIGURE 3: ESR spectra of 16-doxylstearate at 9 °C in (A) DPPG only, (B) DPPG plus 20 mol % PMB, and (C) DPPG plus 20 mol % PMBN.

As shown in Figure 4B, this motional restriction of 16-doxylstearate in PMBN–DPPG was not maintained until the temperature of the main phase transition detected by calorimetry and also detected by a large increase in motion and disorder of the spin-label at 42 °C. The motion of the spin-label increased at 25 °C until it was only a little less than that in the pure lipid, suggesting that the lipid may have transformed into a noninterdigitated gel phase at a temperature well below the temperature of the gel to liquid-crystalline phase transition. Similar behavior had been reported earlier for PMB (Boggs & Rangaraj, 1985). However, as shown in Figure 4B, the increase in motion of the spin-label occurs at a lower temperature for PMBN than for PMB. The fact that calorimetry does not detect a transition at a temperature below the main transition for PMBN–DPPG indicates that this change of motion is not associated with a cooperative melting or refreezing of the chains. However, it may be responsible for the change in fluorescence anisotropy of DPH observed at temperatures below the phase transition temperature of the pure lipid (Figure 2B).

Both PMB and PMBN also caused significant motional restriction of a fatty acid labeled closer to the bilayer–aqueous interface, 5-doxylstearate, in the gel phase of DPPG, as shown in Figure 4A. In contrast to effects seen on DPH and 16-doxylstearate, no significant increase in motion of 5-doxylstearate occurred until the temperature of the transition detected by calorimetry for PMBN–DPPG. In the case of PMB–DPPG, this increase in motion of 5-doxylstearate occurred at the temperature of the higher temperature transition detected by calorimetry.

In the liquid crystalline phase, both PMB and PMBN caused a small decrease in motion (increase in τ_0) of 16-doxylstearate and a large increase in T_{max} and the order parameter for 5-doxylstearate (Figure 4A,B). The effect of PMBN on 5-doxylstearate was a little less than that of PMB.

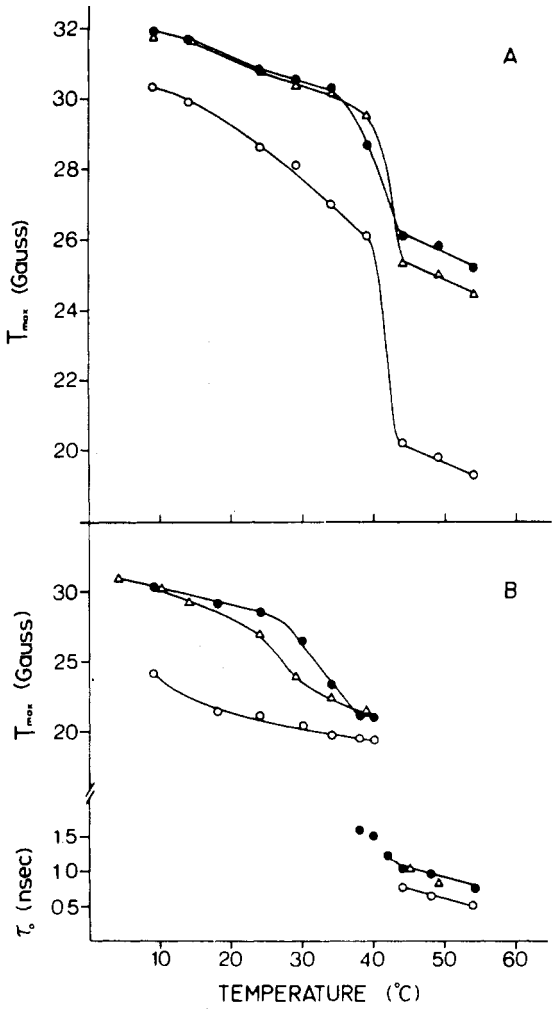

FIGURE 4: Effect of temperature on ESR spectral parameters of (A) 5-doxylstearate and (B) 16-doxylstearate in DPPG (open circles), DPPG–20 mol % PMB (closed circles), and DPPG–20 mol % PMBN (triangles). Note that there is a change in scale in (B) from T_{max} at low temperatures to τ_0 at high temperatures since the motion of this spin-label changes from relatively anisotropic to relatively isotropic at the main gel to liquid-crystalline phase transition temperature. At 35–40 °C, there are two components present in the spectrum for PMB–DPPG as indicated by two points on the graph at each temperature within this range.

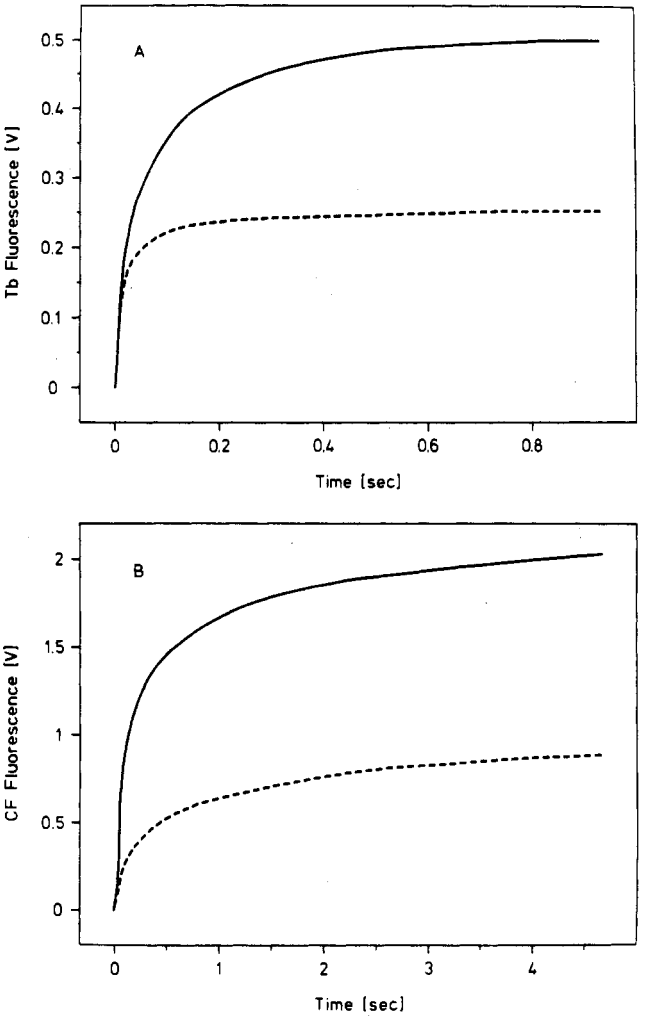

FIGURE 5: PMB-induced (solid line) and PMBN-induced (dashed line) fusion (A) and leakage (B) of small unilamellar PS vesicles. 20 mol % peptide was mixed with CF vesicles (B) or a 1:1 mixture of Tb and DPA vesicles (A) in a stopped-flow apparatus, and the time course of Tb–DPA or CF fluorescence was monitored.

These effects on the fatty acid spin-labels in the liquid-crystalline phase are greater than those on DPH.

Fusion and Leakage Assays. The kinetics of membrane fusion mediated by polymyxin B and PMBN were studied at 22 °C in stopped-flow experiments by mixing solutions of cationic peptide with dispersions of phospholipid vesicles encapsulated either with $TbCl_3$, dipicolinic acid (DPA), or 5-carboxyfluorescein (CF). In these fluorescence assays developed by Wilschut et al. (1980, 1981), the formation of the fluorescent Tb–DPA complex indicates membrane fusion, and the release of CF indicates membrane leakage.

The stopped-flow experiments revealed that both PMB and PMBN induced the fusion of small unilamellar PS vesicles (Figure 5) and of large unilamellar DPPA–DSPC vesicles (Figure 6). The apparatus allowed resolution of the time course of membrane fusion and leakage in the time range from milliseconds to minutes. The background of spontaneous leakage in the absence of multivalent ions was below the limit of detection when small PS vesicles were used. The mixing of large vesicles with buffer released some carboxyfluorescein which amounted to about 10% of the PMB-induced signal. These control experiments demonstrate that the kinetics of vesicle fusion and leakage can be investigated by the stopped-flow technique provided appropriate mixing chambers are used.

Both PMB and PMBN promoted vesicle fusion and leakage; however, their action was quantitatively different. The threshold concentration of 6–7 mol % PMB for the initiation of fusion of PS vesicles was about 5 mol % lower than that of PMBN (Figure 7A). The Tb–DPA fluorescence plateaued at 20 mol % peptide antibiotic. PMB induced a 2-fold higher maximum amplitude than PMBN (Figure 7A). According to the relation

$$F_{rel} = 1 - 0.5^{n-1}$$

the percentage of fused vesicles which displays Tb–DPA fluorescence increases from 50% in the dimer stage to 75% and 87.5% in the trimer and tetramer stages, respectively, and to nearly 100% in the n-mer stage ($n > 6$). The fact that the maximum fluorescence caused by PMBN and PMB differed by a factor of 2 indicates that PMBN mediated mainly the formation of dimers, while PMB induced multiple consecutive fusion events.

Membrane leakage was monitored by the release of encapsulated self-quenched carboxyfluorescein. The CF fluorescence in the presence of 20 mol % and greater PMBN was equivalent to the signal obtained by the treatment of

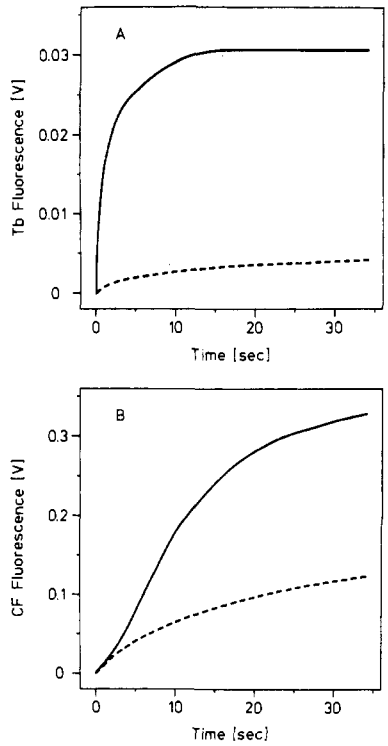

FIGURE 6: PMB-induced (solid line) and PMBN-induced (dashed line) fusion (A) and leakage (B) of large unilamellar DPPA–DSPC vesicles (1:1 mixture, w/w). 20 mol % peptide was mixed with CF vesicles (B) or a 1:1 mixture of Tb and DPA vesicles (A) in a stopped-flow apparatus, and the time course of Tb–DPA or CF fluorescence was monitored.

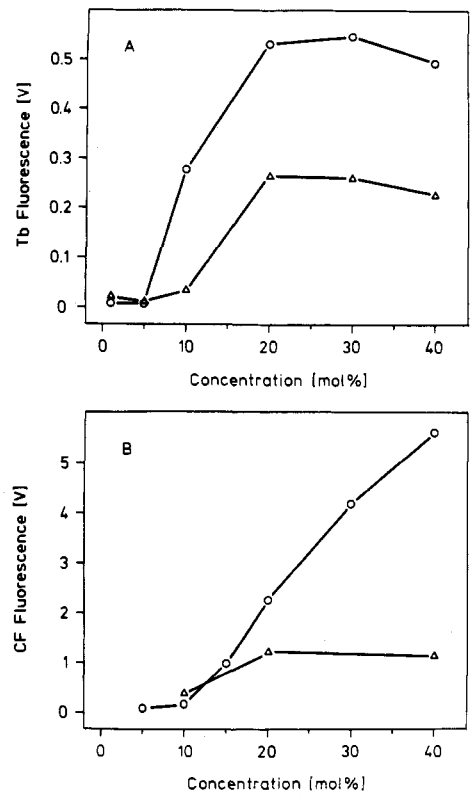

FIGURE 7: Dependence of PS vesicle fusion (A) and leakage (B) on the PMBN (triangles) and PMB (circles) concentration. The maximum signal of Tb (A) and of CF (B) fluorescence is plotted as a function of peptide concentration.

vesicles with 0.1% (v/v) Triton X-100. According to Wilschut et al. (1981), the fluorescence intensity, obtained after disruption of vesicles by addition of 0.1% Triton, can be taken as the value for 100% release of CF into the aqueous environment. Interestingly, the treatment of vesicles with PMB yielded higher fluorescence intensities than that with Triton. Between 10 and 40 mol % PMB, the CF fluorescence monotonously increased; at 40 mol % PMB, the signal was 5–6-fold higher than that obtained by treatment with detergent (Figure 7B). We assume that the carboxyfluorescein fluoresced so strongly because it was trapped by the stacks of phospholipid lamellae which were formed as a consequence of PMB treatment. These stacks of bilayers were regularly seen in the freeze–fracture replicas of specimens treated with PMB (see below).

Table III: PMB- and PMBN-Induced Aggregation and Fusion of Small Unilamellar Phosphatidylserine and of Large Unilamellar DPPA–DSPC Vesicles at 22 °C

	aggregation rate constant (M^{-1} s^{-1})	fusion rate constant (s^{-1})
(A) Small PS Vesicles		
10 mol % PMB	$(3 \pm 2) \times 10^9$	100 ± 40
20 mol % PMB	$(4 \pm 2) \times 10^9$	150 ± 40
30 mol % PMB	$(5 \pm 2) \times 10^9$	200 ± 50
40 mol % PMB	$(5 \pm 2) \times 10^9$	250 ± 50
10 mol % PMBN	$(1 \pm 0.5) \times 10^6$	1.0 ± 0.3
20 mol % PMBN	$(5 \pm 2) \times 10^9$	400 ± 100
30 mol % PMBN	$(4 \pm 2) \times 10^9$	500 ± 200
40 mol % PMBN	$(5 \pm 2) \times 10^9$	400 ± 150
(B) Large DPPA–DSPC Vesicles		
20 mol % PMB	$(5 \pm 2) \times 10^8$	10 ± 3
20 mol % PMBN	$(4 \pm 2) \times 10^8$	3 ± 1

The rate constants of vesicle aggregation and fusion were evaluated from the experimental curves according to the theory developed by Bentz et al. (1983a). Above the threshold value, the PMB- and PMBN-mediated aggregation of vesicles turned out to be a diffusion-controlled process (Table III). The small PS vesicles fused with a frequency of 10^2–(5×10^2) s^{-1} and the large DPPA–DSPC vesicles with a frequency of 1–10 s^{-1} (Table III). The ratio of the f_{11} values for small and large vesicles approximately corresponds with the reciprocal ratio of the number of molecules which make up one vesicle. This result provides evidence that the elementary kinetic steps of single molecules take place within the same period of time in large and small vesicles. It follows that the kinetic behavior of pure PS and of the DPPA–DSPC mixture did not differ significantly from each other. Hence, besides its negative charge, the configuration of the head group of an acidic phospholipid does not seem to be of importance for the rates of aggregation and fusion caused by PMB and PMBN.

Freeze–Fracture Electron Microscopy. The freeze–fracture replicas regularly showed that after incubation with PMB or PMBN, the liposomes were aggregated, large, and multilamellar. These morphological alterations which were greater with 50 mol % than with 20 mol % peptide were interpreted as the results of fusion and leakage events in correspondence with the data of the fluorescence assays.

After incubation with PMB at 20 °C, the fractured liposome membranes displayed on several successive halves of bilayers a similar patchy distribution of numerous 12–50-nm roundish to oval depressions (Figure 8a), indicating the formation of lipid–polymyxin domains (Hartmann et al., 1978). This finding was independent of fixation and the molar ratio of peptide to lipid. Incubation with PMB at 40 °C led to the collapse and disruption of the vesicles: stacks of bilayers with irregular forms and extensions were seen. The treatment with PMBN at 20 and 40 °C was less membrane perturbing. The shape of the multilamellar liposomes was more preserved, and the cleaved membranes remained smooth. However, if the

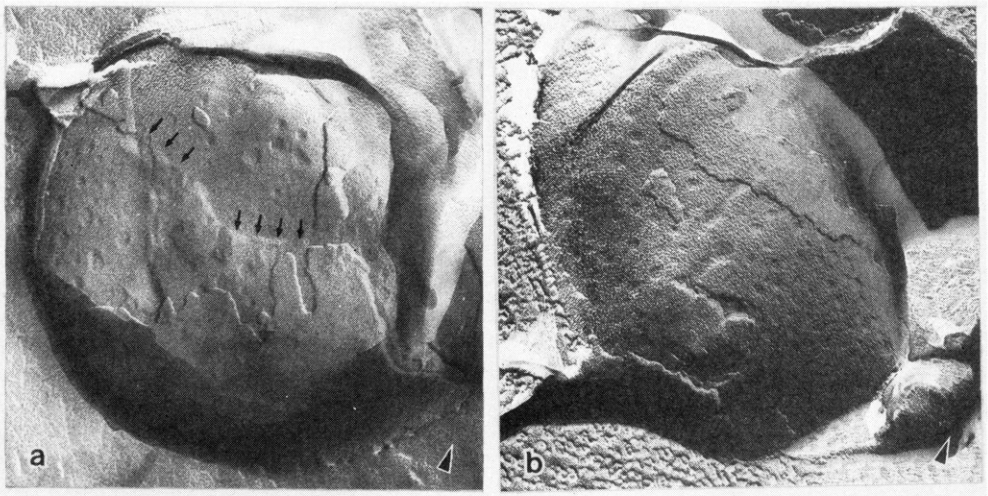

FIGURE 8: Freeze–fracture replicas of large multilamellar liposomes. Samples of a DPPA–DSPC vesicle preparation were incubated at 20 °C for 20 min with 20 mol % PMB (a) or 20 mmol % PMBN (b) and subsequently fixed. The arrows in (a) point to fusion sites where the usually well-defined border between two cleaved bilayers became indistinct or even disappeared. The arrowhead gives the direction of shadowing. (a and b) 40000×.

sample was fixed after incubation, at least the cleaved membrane showed depressions which were similar to those produced by treatment with PMB; their size was more uniform (about 25 nm in diameter) (Figure 8b).

Discussion

This paper compares the action of polymyxin B and polymyxin B nonapeptide on model membranes of the acidic phospholipids phosphatidic acid, phosphatidylserine, and phosphatidylglycerol. Polymyxin B has been used by several authors as a model compound for the study of peptide–lipid interactions (Hartmann et al., 1978; Sixl & Galla, 1979, 1982; El Mashak & Tocanne, 1980; Ranck & Tocanne, 1982; Gad, 1983; Mushayakarara & Levin, 1984; Theretz et al., 1984; Boggs & Rangaraj, 1985; Sixl & Watts, 1985). In the following paragraphs, we relate the literature and our own data obtained from studies on model membranes in vitro to the physiological action of PMB and PMBN on bacteria in vivo. The data can help us to understand why the closely related compounds PMB and PMBN act so differently on the membranes of Gram-negative bacteria.

In general terms, the antibiotic polymyxin B turned out to be more membrane perturbing than its nonbactericidal derivative PMBN. Both compounds promoted the fusion of vesicles of acidic phospholipids at comparable rates. However, as demonstrated by the fusion and leakage assays and the freeze–fracture replicas, PMB disrupted the vesicles and induced the formation of multilamellar coacervates, whereas in the presence of PMBN the vesicular structure was more preserved. As revealed by fluorescence polarization (Sixl & Galla, 1979), Raman spectroscopy (Mushayakarara & Levin, 1984), and NMR spectroscopy (Sixl & Watts, 1985), the interaction of polymyxin B with charged bilayers leads to domain formation through lateral phase separations. Their visualization in freeze–fracture replicas required no fixation, suggesting that the exchange of phospholipids between PMB complexes and the bulk lipid matrix occurred considerably slower than the freezing of the samples which took place within some tenths of a second. The PMB–lipid domains were seen on several successive bilayers, suggesting transbilayer redistribution of PMB. The translocation and disruption of bilayers of model membranes by polymyxin B fit into the generally accepted picture of PMB action on Gram-negative bacteria, where polymyxin B translocates through the outer membrane and subsequently disrupts the inner cytoplasmic membrane.

In the case of PMBN, the lipid–peptide domains were seen on only one side of the DPPA–DSPC bilayer and not in successive ones, presumably because only half of the membrane was permeated by PMBN. In addition, since fixation with glutaraldehyde was necessary for the visualization of lipid–PMBN domains, we conclude that PMBN rapidly exchanges between the bulk solution and its binding sites on the outer side of the membrane and that phase separation, if it occurs at all, has to take place on a fast time scale.

The equilibrium experiments demonstrated further differences between PMB and PMBN. As shown by DPH fluorescence anisotropy, PMB slightly restricted the rotational mobility of DPH in DPPG and DPPA in the liquid-crystalline phase, but the addition of PMBN had no effect (Figure 2). Titration of DPPA with polymyxin B revealed a cooperative binding curve (Sixl & Galla, 1979); our analogous experiment with PMBN gave no evidence for cooperativity.

In contrast to results with DPH, both PMB and PMBN decreased the motion and/or increased the order of fatty acid spin-labels in the liquid-crystalline phase of DPPG. The magnitude of the effect depended on the location of the probe within the bilayer, with a much greater effect felt close to the bilayer–aqueous interface than toward the center of the bilayer. This may explain why DPH gave different results; DPH may be located in the center of the bilayer (Seelig, 1977; Kinosita et al., 1981). The much greater effect of PMB and PMBN on 5-doxylstearate compared to 16-doxylstearate in the liquid-crystalline phase suggests that they penetrate partway into the bilayer. Similar results have been observed for myelin basic protein, an extrinsic protein which binds electrostatically but has hydrophobic residues which may penetrate partway into the bilayer (Boggs, 1984). The similar effects of PMBN and PMB on 5-doxylstearate indicate that the fatty acid tail of PMB is not necessary and that penetration of individual hydrophobic side chains of amino acids of PMBN is sufficient to restrict the motion of 5-doxylstearate.

The large motional restriction of 16-doxylstearate in the gel phase caused by both PMB and PMBN suggests that PMBN, like PMB, causes interdigitation in the gel state. Similar behavior occurs with the methyl ester of 16-doxylstearate (Boggs & Rangaraj, 1985) and with a phosphatidylglycerol spin-label, indicating that it is not an artifact related to the fatty acid spin-label. This degree of gel phase immobilization

of spin-labeled chains, where the spin-label is located near the apolar end of the chain, is unusual. It also occurs in interdigitated phases of asymmetric chain length forms of phosphatidylcholine (Boggs & Mason, 1987). These lipids have been shown by X-ray diffraction to be interdigitated (Hui et al., 1984; McIntosh et al., 1984). X-ray diffraction studies have also shown that interdigitation of symmetric chain length lipids often occurs at high concentrations of amphipathic compounds, which penetrate partway into the bilayer (McIntosh et al., 1983), and compensates for the otherwise disordering effect such compounds would have. The similar ability of PMB and PMBN to cause interdigitation, as inferred from their effects on fatty acid chain motion, indicates that penetration of hydrophobic side chains from a peptide bound electrostatically on the surface is sufficient to induce this phenomenon. Immobilization was maintained to a higher temperature in the presence of PMB than PMBN, however, suggesting that PMB may maintain interdigitation better than PMBN. This may be due to the slower rate of exchange for PMB or to its greater penetration as a result of its acyl chain.

PMB and PMBN have much greater effects on the transition temperature of DPPA than DPPG. However, the transition temperatures of the PMB-bound and PMBN-bound DPPAs are very similar to those of the PMB-bound and PMBN-bound DPPGs, indicating that both lipids are in a similar state when bound to PMB or PMBN. The large decrease for DPPA is a result of loss of its intermolecular hydrogen bonding interactions when PMB or PMBN binds to its hydrogen bond accepting phosphate sites. This causes it to behave similarly to DPPG. PMB causes two phase transitions in both DPPA (disregarding the highest one due to uncomplexed DPPA) and DPPG while PMBN causes only one. The lowest temperature transition for PMB-bound DPPA was earlier concluded to be a result of PMB bound only hydrophobically and the second higher temperature transition, a result of both electrostatic and hydrophobic interactions (Sixl & Galla, 1982). The fact that PMBN causes only one transition at a similar temperature as the second higher one for PMB lends support to this suggestion. A similar mechanism may then be responsible for the two phase transitions in PMB–DPPG compared to the single one in PMBN–DPPG.

The ability of polymyxins to cause interdigitation of phosphatidylglycerol bilayers may be of importance for their physiological effects on the membranes of Gram-negative bacteria. PG is the major anionic phospholipid in the cell envelope. Although interdigitation has so far been found to occur only in the gel phase, a substantial proportion of the PG in bacterial membranes contains saturated fatty acids (Hammond et al., 1984) and therefore may be able to form gel phase domains. The critical role of phosphatidylglycerol for the action of PMB and PMBN on bacterial membranes becomes evident during adaptation and acquisition of resistance to polymyxin [see Gilleland et al. (1984) and references cited therein]. Upon exposure to polymyxin, susceptible *Pseudomonas aeruginosa* strains adapt to polymyxin and acquire resistance by rapid alteration of the cell envelope. The PG content decreases from 20–25% of the membrane lipid to zero (Gilleland et al., 1984). This experimental finding implies that PG is a target of PMB action in vivo. Hence, it is conceivable that PMB-induced interdigitation of some domains of gel-state lipid containing saturated chains in the inner membrane might be involved in its bactericidal effect through an increase in permeability, particularly at the interface between interdigitated and noninterdigitated domains.

Although PMBN can cause interdigitation in lipid vesicles when it is present on both sides of the membrane, it would not be likely to do so in bacteria since it does not translocate to the other side of the membrane. However, the fact that it is able to cause interdigitation in lipid vesicles indicates that its amino acid side chain can penetrate partway into the bilayer. This would have a disordering effect in the absence of the stabilizing effect of interdigitation and could cause the permeability of the bilayer to other antibiotics to increase. Similarly, if PMB is unable to cause interdigitation in bacterial membranes at physiological temperatures, its bactericidal effect may be related to its disordering effect on the lipid, which is greater than that of PMBN, and its ability to translocate across the outer membrane and enter the inner membrane.

In addition to phospholipid, the other constituents of the outer membrane, i.e., LPS and protein, may contribute to the $(1–2) \times 10^6$ PMBN binding sites per cell (Vaara & Viljanen, 1985). Among the proteins, the porins serve as nonspecific channels through the outer membrane. However, it is highly unlikely that PMBN affects porin-mediated transport to a significant extent because the nonapeptide only slightly sensitized Gram-negative bacteria to compounds such as lincomycin and cloxacillin (Table I) which penetrate the outer membrane through porin pores (Viljanen & Vaara, 1984). However, other outer membrane proteins are certainly involved in PMBN action. If *Pseudomonas aeruginosa* strains are grown under magnesium depletion (Brown & Melling, 1969; Anwar et al., 1983), the bacteria become resistant to polymyxin B (Nicas & Hancock, 1980), and the PMBN-mediated sensitization to the hydrophobic antibiotics fusidic acid and erythromycin is lost (own unpublished data). In parallel, the protein pattern of the cell envelope changes, suggesting that PMB and PMBN share a set of common protein binding sites.

In addition to proteins and acidic phospholipids, the LPS as a major target of PMB and PMBN action has to be considered. Lipopolysaccharides possess cation binding sites which noncovalently cross-bridge adjacent LPS molecules [see recent reviews by Hammond et al. (1984), Hancock (1984), and Nikaido and Vaara (1985)]. Fluorescence titrations of dansylated LPS with PMB revealed a high-affinity binding site of $K = 2 \times 10^6$ M^{-1} (Schindler & Osborn, 1979) which is slightly higher than the values reported for bacterial phospholipids of $K = (2–4) \times 10^5$ M^{-1} (Storm et al., 1977). The interaction of PMBN with LPS was demonstrated by indirect bioassays (Vaara, 1983) and displacement titrations with an ESR probe (Peterson et al., 1985). Comparing PMB and PMBN, the removal of the acyl chain reduced the affinity of the compound for LPS to values close to those of similarly charged cations (Peterson et al., 1985).

Our own results are indicative of a rather nonspecific electrostatic interaction between LPS and PMBN. Absorption and circular dichroism spectra of a mixture of LPS and PMBN were a superposition of the spectra of the individual compounds (data not shown). In the NMR spectrum, the addition of LPS to PMB or PMBN induced signal broadening without any detectable shift of the resonances. The changes of the NMR spectrum indicate the immobilization of peptide and LPS in the complex, confirming the results of Peterson et al. (1985), who observed the rigidification of LPS in the complex by ESR data. PMB immobilized LPS more strongly than its nonapeptide derivative. The evaluation of the NMR titrations yielded an apparent binding constant of about 10^5 M^{-1} for the LPS–PMBN complex which within experimental error corresponds to the stability constant of the phosphatidic acid–

PMBN complex (see Results).

Taking the literature and our own data together, the following picture about the action of PMB and PMBN on the cell envelope of Gram-negative bacteria emerges: Polymyxin B and polymyxin B nonapeptide bind to the same sites on the outer bacterial membrane, thereby inducing an increase of outer membrane permeability. PMB crosses the outer membrane and subsequently disrupts the cytoplasmic membrane, possibly by causing interdigitation of some domains of gel phase lipid containing saturated chains. In contrast, PMBN has access only to the surface of the cell envelope, and hence its action is confined to sensitization of the cell envelope to other hydrophobic compounds.

ACKNOWLEDGMENTS

We thank Godha Rangaraj for her collaboration in the calorimetric and ESR experiments and Maria Wehsling for her aid in the sensitivity determinations.

REFERENCES

Anwar, H., Lambert, P. A., & Brown, M. R. W. (1983) *Biochim. Biophys. Acta 761*, 119–125.

Bader, J., & Teuber, M. (1973) *Z. Naturforsch., C: Biochem., Biophys., Biol., Virol. 28C*, 422–430.

Barrow, D. A., & Lentz, B. R. (1980) *Biochim. Biophys. Acta 597*, 92–99.

Bearer, E. L., & Friend, D. S. (1980) *Proc. Natl. Acad. Sci. U.S.A. 77*, 6601–6605.

Bearer, E. L., Düzgünes, N., Friend, D. S., & Papahadjopoulos, D. (1982) *Biochim. Biophys. Acta 693*, 93–98.

Bentz, J., Nir, S., & Wilschut, J. (1983a) *Colloids Surf. 6*, 333–363.

Bentz, J., Düzgünes, N., & Nir, S. (1983b) *Biochemistry 22*, 3320–3330.

Boggs, J. M. (1983) in *Membrane Fluidity in Biology* (Aloia, R. C., Ed.) Vol. 2, pp 89–130, Academic Press, New York.

Boggs, J. M., & Rangaraj, G. (1985) *Biochim. Biophys. Acta 816*, 221–233.

Boggs, J. M., & Mason, J. T. (1987) *Biochim. Biophys. Acta* (in press).

Boggs, J. M., Stamp, D., & Moscarello, M. A. (1981) *Biochemistry 20*, 6066–6072.

Brown, M. R. W., & Melling, J. (1969) *J. Gen. Microbiol. 54*, 439–444.

Chihara, S., Tobita, T., Yahata, M., Ito, A., & Koyama, Y. (1973) *Agric. Biol. Chem. 37*, 2455–2463.

Cullis, P. R., & Hope, M. J. (1978) *Nature (London) 271*, 672–674.

El Mashak, E. M., & Tocanne, J. F. (1980) *Biochim. Biophys. Acta 596*, 165–179.

Englund, P. T., King, T. P., Craig, L. C., & Walti, A. (1968) *Biochemistry 7*, 163–174.

Fraley, R., Wilschut, J., Düzgünes, N., Smith, C., & Papahadjopoulos, D. (1980) *Biochemistry 19*, 6021–6029.

Gad, A. E. (1983) *Biochim. Biophys. Acta 728*, 377–382.

Galla, H. J., & Trudell, J. R. (1980) *Biochim. Biophys. Acta 602*, 522–530.

Gilleland, H. E., Champlin, F. R., & Conrad, R. S. (1984) *Can. J. Microbiol. 30*, 869–873.

Hammond, S. M., Lambert, P. A., & Rycroft, A. N. (1984) *The Bacterial Cell Surface*, pp 57–111, Croom Helm Ltd., Beckenham, Kent, U.K.

Hancock, R. E. W. (1984) *Annu. Rev. Microbiol. 38*, 237–264.

Hartmann, W., Galla, H. J., & Sackmann, E. (1977) *FEBS Lett. 78*, 169–172.

Hartmann, W., Galla, H. J., & Sackmann, E. (1978) *Biochim. Biophys. Acta 510*, 124–139.

Herrmann, U., Tümmler, B., Maass, G., Koo Tze Mew, P., & Vögtle, F. (1984) *Biochemistry 23*, 4059–4067.

Huang, C. (1969) *Biochemistry 8*, 344–352.

Hui, S. W., Mason, J. T., & Huang, C. (1984) *Biochemistry 23*, 5570–5577.

King, A., Shannon, K., & Philips, J. (1984) *J. Antimicrob. Chemother. 13*, 325–331.

Kinosita, K., Kataoka, R., Kimura, Y., Gotoh, O., & Ikegami, A. (1981) *Biochemistry 20*, 4270–4277.

McIntosh, T. J., McDaniel, R. V., & Simon, S. A. (1983) *Biochim. Biophys. Acta 731*, 109–114.

McIntosh, T. J., Simon, S. A., Ellington, J. C., Jr., & Porter, N. A. (1984) *Biochemistry 23*, 4038–4044.

Mushayakarara, E., & Levin, I. W. (1984) *Biochim. Biophys. Acta 769*, 585–595.

Nicas, T. I., & Hancock, R. E. W. (1980) *J. Bacteriol. 143*, 872–878.

Nikaido, H., & Vaara, M. (1985) *Microbiol. Rev. 49*, 1–32.

Nir, S., Bentz, J., & Wilschut, J. (1980) *Biochemistry 19*, 6030–6036.

Parce, J. W., Henry, N., & McConnell, H. M. (1978) *Proc. Natl. Acad. Sci. U.S.A. 75*, 1515–1518.

Peterson, A. A., Hancock, R. E. W., & McGroarty, E. J. (1985) *J. Bacteriol. 164*, 1256–1261.

Ranck, J. L., & Tocanne, J. F. (1982) *FEBS Lett. 143*, 175–178.

Rosenthal, K. S., Swanson, P. E., & Storm, D. R. (1976) *Biochemistry 15*, 5783–5792.

Schindler, M., & Osborn, M. J. (1979) *Biochemistry 18*, 4425–4430.

Seelig, J. (1977) *Q. Rev. Biophys. 10*, 353–418.

Sixl, F., & Galla, H. J. (1979) *Biochim. Biophys. Acta 557*, 320–330.

Sixl, F., & Galla, H. J. (1980) *Biochem. Biophys. Res. Commun. 94*, 319–323.

Sixl, F., & Galla, H. J. (1982) *Biochim. Biophys. Acta 693*, 466–478.

Sixl, F., & Watts, A. (1985) *Biochemistry 24*, 7906–7910.

Storm, D. R., Rosenthal, K. S., & Swanson, P. E. (1977) *Annu. Rev. Biochem. 46*, 723–763.

Sundler, R., & Papahadjopoulos, D. (1981) *Biochim. Biophys. Acta 649*, 743–750.

Teuber, M., & Bader, J. (1976) *Arch. Microbiol. 109*, 51–58.

Teuber, M., & Miller, J. R. (1977) *Biochim. Biophys. Acta 467*, 280–289.

Theretz, A., Teissie, J., & Tocanne, J. F. (1984) *Eur. J. Biochem. 142*, 113–119.

Thomas, A. H., & Holloway, J. (1978) *J. Chromatogr. 161*, 417–420.

Tümmler, B., Maass, G., Vögtle, F., Sieger, H., Heimann, U., & Weber, E. (1979) *J. Am. Chem. Soc. 101*, 2588–2598.

Vaara, M. (1983) *FEMS Microbiol. Lett. 18*, 117–121.

Vaara, M., & Vaara, T. (1983a) *Antimicrob. Agents Chemother. 24*, 107–113.

Vaara, M., & Vaara, T. (1983b) *Antimicrob. Agents Chemother. 24*, 114–122.

Vaara, M., & Vaara, T. (1983c) *Nature (London) 303*, 526–528.

Vaara, M., & Viljanen, P. (1985) *Antimicrob. Agents Chemother. 27*, 548–554.

Viljanen, P., & Vaara, M. (1984) *Antimicrob. Agents Chemother. 25*, 701–705.
Wilschut, J., Düzgünes, N., Fraley, R., & Papahadjopoulos, D. (1980) *Biochemistry 19*, 6011–6021.
Wilschut, J., Düzgünes, N., & Papahadjopoulos, D. (1981) *Biochemistry 20*, 3126–3133.
Wilschut, J., Nir, S., Scholma, J., & Hoekstra, D. (1985) *Biochemistry 24*, 4630–4636.

Oxygen Equilibrium Studies of Cross-Linked Asymmetrical Cyanomet Valency Hybrid Hemoglobins: Models for Partially Oxygenated Species†

Shigetoshi Miura,‡,§ Masao Ikeda-Saito,‖ Takashi Yonetani,‖ and Chien Ho*,‡
Department of Biological Sciences, Carnegie Mellon University, Pittsburgh, Pennsylvania 15213, and Department of Biochemistry and Biophysics, University of Pennsylvania School of Medicine, Philadelphia, Pennsylvania 19104-6089
Received March 21, 1986; Revised Manuscript Received October 24, 1986

ABSTRACT: Oxygen equilibrium curves have been measured to determine the binding constant at each oxygenation step (K_i) for various cross-linked hemoglobins, $(\alpha\beta)_A(\alpha\beta)_C$XL, $(\alpha^{+CN}\beta)_A(\alpha\beta)_C$XL, $(\alpha\beta^{+CN})_A(\alpha\beta)_C$XL, $(\alpha^{+CN}\beta^{+CN})_A(\alpha\beta)_C$XL, and $(\alpha\beta^{+CN})_A(\alpha^{+CN}\beta)_C$XL, where the subscripts A and C denote that the $\alpha\beta$ dimer is derived from human normal adult hemoglobin and mutant hemoglobin C (β6Glu → Lys), respectively, and XL denotes cross-linking between the lysyl residues at position 82 in the two β chains by bis(3,5-dibromosalicyl) fumarate as described by Miura and Ho [Miura, S., & Ho, C. (1982) *Biochemistry 21*, 6280–6287]. The oxygen equilibrium data indicate that the oxygen affinity increases with the number of cyanomet hemes carried by the cross-linked mixed valency hybrid hemoglobins. The oxygen binding property depends not only on the number of the subunits carrying cyanomet hemes but also on the distribution of cyanomet hemes among the four subunits. A striking effect is observed in singly cyanomet valency hybrid hemoglobins; namely, $(\alpha^{+CN}\beta)_A(\alpha\beta)_C$XL exhibits lower oxygen affinity and higher cooperativity than $(\alpha\beta^{+CN})_A(\alpha\beta)_C$XL. The magnitude of the Adair constants and their pH dependency of $(\alpha^{+CN}\beta)_A(\alpha\beta)_C$XL ($K_i$, i = 1–3) are analogous to those of the Adair constants of $(\alpha\beta)_A(\alpha\beta)_C$XL ($K_i$, i = 2–4), whereas such an analogy is not observed between $(\alpha\beta^{+CN})_A(\alpha\beta)_C$XL and $(\alpha\beta)_A(\alpha\beta)_C$XL. The doubly cyanomet mixed valency hybrid cross-linked hemoglobins exhibit high oxygen affinity and reduced cooperativity, and their Adair constants are not analogous to K_3 and K_4 of $(\alpha\beta)_A(\alpha\beta)_C$XL. The present results on the oxygen binding properties of cross-linked mixed valency hybrid hemoglobins provide additional support to the conclusion based on a previous proton nuclear magnetic resonance investigation of these hybrid hemoglobins that there are at least three functional and energetically important structures of hemoglobin in going from the deoxy to the ligated state. Thus, the cooperative oxygenation process of human normal adult hemoglobin cannot be simply described by two-structure allosteric models.

In spite of the large amount of research during the last several decades, the molecular mechanism of cooperative oxygen binding by hemoglobin (Hb)[1] is not yet fully understood. The cooperativity arises from the reversible transition between fully ligated and fully deoxy forms of human normal adult hemoglobin (Hb A), whose structures have been determined by X-ray crystallography [for example, see Baldwin (1980), Shaanan (1983), and Fermi et al. (1984)]. One of the most challenging tasks in current Hb research is to describe the structural change induced at each oxygenation step by characterizing the properties of the intermediate ligated species, namely, Hb A with one, two, and three ligand molecules bound within a tetramer, and comparing them with the properties of the fully deoxy and ligated species, and thus to be able to interpret alterations in functional properties in terms of molecular structural changes. Because at any given fractional saturation between the fully deoxy and fully oxy states, various molecular species with binding of zero to four ligand molecules coexist as a statistical mixture, it is not feasible to isolate a stable intermediate ligation state by using Hb A. (This difficulty in studying the intermediate ligation states is not due to the Hb A itself but rather to the use of O_2 as the ligand.) The cooperative nature of oxygen binding further reduces the relative populations of intermediate ligated states to a small fraction in comparison with those of fully deoxy and ligated forms. Thus, the majority of the information available about the properties of the Hb molecule has been unfortunately limited to either the fully ligated or the fully deoxy form of

† This work was supported by research grants from the National Institutes of Health (HL-24525 to C.H., AI-20463 to M.I.-S., HL-14508 to T.Y.) and from the National Science Foundation (PCM 83-16935 to T.Y.).
* Address correspondence to this author.
‡ Carnegie Mellon University.
§ Present address: Institute for Developmental Research, Aichi Prefectural Colony, Kamiya-cho, Kasugai, Aichi 480-03, Japan.
‖ University of Pennsylvania School of Medicine.

[1] Abbreviations: Hb, hemoglobin; Hb A, human normal adult hemoglobin; met-Hb, methemoglobin; α^{+CN} or β^{+CN}, α or β subunit containing heme iron that is in the ferric state and is combined with cyanide; $(\alpha\beta)_A(\alpha\beta)_C$XL, cross-linked Hb, where the subscripts A and C denote that the $\alpha\beta$ dimer comes from Hb A and Hb C, respectively, and XL denotes cross-linked Hb; $\alpha(Fe)_2\beta(Co)_2$, hybrid Hb containing iron protoporphyrin IX in the α subunits and cobaltous protoporphyrin IX in the β subunits; $\alpha(Co)_2\beta(Fe)_2$, hybrid Hb containing cobaltous protoporphyrin IX in the α subunits and iron protoporphyrin IX in the β subunits; NMR, nuclear magnetic resonance; n, Hill coefficient; DPG, 2,3-diphosphoglycerate; IHP, inositol hexaphosphate; RMS, root mean square.

0006-2960/87/0426-2149$01.50/0